Catalysis Today 146 (2009) 148–153

Contents lists available at ScienceDirect

Catalysis Today

journal homepage: www.elsevier.com/locate/cattod

Performance of $La_{1-x}Ce_xFe_{0.7}Ni_{0.3}O_3$ perovskite catalysts for methane steam reforming

Sang Ok Choi, Sang Heup Moon *

School of Chemical & Biological Engineering and Institute of Chemical Processes, Seoul National University, San 56-1, Shillim-dong, Kwanak-ku, Seoul 151-744, Republic of Korea

ARTICLE INFO

Article history:
Available online 25 March 2009

Keywords:
Perovskite
Calcination temperature
Ce-substitution
Steam reforming
Hydrogen
Methane

ABSTRACT

$La_{1-x}Ce_xFe_{0.7}Ni_{0.3}O_3$ perovskite catalysts, denoted as LCFN-x ($0.1 \leq x \leq 0.5$), were prepared using a Pechini method. The effects of Ce-substitution and calcination temperature on the structure and performance of the prepared catalysts during the steam reforming of methane (SRM) were investigated. The XRD patterns of these catalysts indicated that a well-crystallized perovskite structure was formed when LFN and LCFN were calcined at temperatures higher than 500 and 600 °C, respectively. For the reaction system investigated in this study, the most suitable calcination temperature was 700 °C. The 700 °C-calcined catalysts, denoted as LFN-700 and LCFN-700, exhibited the highest methane conversion among catalysts of the same type, due to their relatively large surface area and small crystallite size compared with those of perovskite catalysts. The catalytic activity increased with the amounts of added Ce, up to x = 0.2–0.3, but decreased significantly when $x \geq 0.5$. In particular, LCFN-0.2 exhibited a higher hydrogen yield and slower deactivation rates than those exhibited by a commercial catalyst at the steam/carbon ratio of 1. This result was obtained because coke deposition was retarded to a greater extent on LCFN-0.2 than on the commercial catalyst under the selected reaction conditions.

1. Introduction

Steam reforming of methane (SRM) is a promising method for hydrogen production due to the high hydrogen/carbon ratio of methane and an established infrastructure required for the adoption of the process [1–3]. Even though Ni catalysts are generally used in the SRM process due to their high catalytic activity, these catalysts are easily deactivated by coke deposition on the surface during the reaction [4–6]. Thus, to reduce coke deposition, SRM is commonly performed using a high steam/carbon (S/C) ratio in the reactant stream, which also leads to higher conversion rates [7,8]. However, a high S/C ratio is not energetically favorable due to the generation of steam in excess of that required by the reaction stoichiometry, which dilutes the hydrogen concentration in reformate gases [7,9]. Due to the disadvantages of using a high S/C ratio, development of catalysts with high activity and minimal coke deposition under the condition of a low S/C ratio is needed.

Perovskite oxides (ABO_3), which contain rare-earth and transition metals as the A- and B-site cations, respectively, have been studied as catalysts for the production of syngas from hydrocarbons [10–20]. Reportedly, the B-site metal in perovskite oxide forms the primary active site, while the A-site metal has a strong effect on the stability and potentially improves the catalytic performance via an interaction with the B-site metal [13,21,22]. La, a rare-earth metal, and Fe, a transition metal, are generally used as the A- and B-site metals, respectively, in reforming reactions because they have high thermal stability [13,17,23]. It is well known that perovskite oxides, including $LaFeO_3$, can be prepared by many different methods, such as the Pechini method [19,24,25], aqueous combustion synthesis [12,13,15,18], a solid mixing method [16] and a sol–gel method using pionic acid [17]. As the calcination temperature in the final step of the preparation procedure is varied from 600 to 800 °C in each preparation method, it is important to investigate the effect of calcination temperature on the performance and structure of the final catalyst.

It has been reported that partially substituted $LaFe_{1-x}Ni_xO_3$ (LFN) exhibits high activity in the SRM. In particular, $LaFe_{0.7}Ni_{0.3}O_3$ shows the best catalytic performance [17] and the partial replacement of Ce in $La_{1-x}Ce_xNiO_3$ enhances the catalytic activity and inhibits coke formation during the dry reforming of methane [14].

In this study, $La_{1-x}Ce_xFe_{0.7}Ni_{0.3}O_3$ (LCFN-x) perovskite was prepared by the Pechini method by varying the calcination temperature and the degree of Ce-substitution. The LCFN-x was characterized by N_2-physisorption, X-ray diffraction (XRD), temperature-programmed reduction (TPR), elemental analysis (EA) and transmission electron microscopy (TEM). The perfor-

* Corresponding author. Tel.: +82 2 880 7409; fax: +82 2 875 6697.
E-mail address: shmoon@surf.snu.ac.kr (S.H. Moon).

0920-5861/$ – see front matter © 2009 Elsevier B.V. All rights reserved.
doi:10.1016/j.cattod.2009.02.023

mance of the prepared, heat-treated catalysts in the SRM was compared with that of a commercial catalyst (COM).

2. Experimental

2.1. Preparation of catalysts

$La_{1-x}Ce_xFe_{0.7}Ni_{0.3}O_3$ perovskite catalysts, denoted as LCFN-*x*, were prepared by a Pechini method [24], *x* ranging between 0.1 and 0.5. Here, *x* represents the nominal amounts of Ce, in the unit of Ce/(La + Ce) atomic ratio, added in the catalyst preparation step. A Ce-free catalyst (LFN) and a La-free catalyst (CFN), i.e., $x = 0$ and 1, respectively, were also prepared for comparison. Metal nitrates, the amounts of which were adjusted to meet the nominal contents of LFN, CFN and LCFN-*x* catalysts, were dissolved in distilled water. Subsequently excess amounts of citric acid and ethylene glycol were added to the solution. The resulting solution was stirred for 7 h and then evaporated in air at 70 °C for approximately 5 h until a gel-like material formed. The gel-like material was crushed into a powder, decomposed in air at 400 °C for 2 h, and finally calcined at temperatures between 500 and 900 °C for 6 h for structural rearrangement. The samples were labeled as LFN- and LCFN-*y*, where $y = 500$, 600, 700, 800 and 900.

2.2. Characterization

The BET surface areas of prepared and commercial catalysts were measured by N_2-physisorption using an ASAP2010 (Micromeritics). Prior to the measurements, a reactor containing the sample catalyst was evacuated at 200 °C for 1 h to remove both impurities and water from the catalyst surface. XRD patterns were obtained on a diffractometer (MAC science Co.) using Cu Kα radiation. XRD profiles were collected in the 2θ range, 10–80°, in steps of 10°/min. The catalyst phases were identified by comparing the observed results with the JCPDS database. TPR was performed in a BELCat-B (BEL, Japan) equipped with a thermal conductivity detector to investigate the reduction properties of the catalysts. Before TPR, catalysts were pre-treated in Ar at 120 °C for 1 h to remove both impurities and water from the surface. The TPR experiment was conducted in a 5 mol% H_2/Ar stream flowing at a rate of 20 ml/min, while the temperature was raised from 30 to 800 °C at a rate of 10 °C/min. CO uptake was measured using a pulse injection method. Before the measurements, the catalyst was reduced in 5 mol% H_2/Ar at 700 °C for 1 h. The measurement was finished when the difference in areas among the last three CO-pulse injection peaks was less than 1%.

2.3. Catalytic activity

The powder catalyst was used for the SRM, which was carried out in a U-shaped quartz micro-reactor at atmospheric pressure and at different reaction temperatures ranging from 500 to 800 °C. For comparison, a COM containing 10–14 wt.% of NiO and 86–90 wt.% of Al_2O_3 was also tested for SRM under the same reaction condition. The reactant mixture, in which the S/C ratio was changed from 1 to 3, was fed into the reactor containing 50 mg of the sample catalyst at a flow rate of 90 ml/min. GHSV was 86,400 h^{-1}. Prior to the activity test, the sample catalyst was reduced in H_2/N_2 at 700 °C for 1 h and then the catalyst was cooled in N_2 to 500 °C. The reaction products were analyzed with an on-line G.C. (Agilent, model 6890 series with a TCD) using a packed column (Supelco, Carbosieve II 100/120 mesh). The CH_4 conversion was calculated based on carbon balance and the H_2 fraction in dry gas was obtained after water was removed from the product stream:

$$CH_4 \text{ conversion } (\%) = \frac{F_{CO,out} + F_{CO_2,out}}{F_{CH_4,out} + F_{CO,out} + F_{CO_2,out}} \times 100 \quad (1)$$

$$H_2 \text{ fraction in dry gas } (\%) = \frac{F_{H_2,out}}{F_{H_2,out} + F_{CH_4,out} + F_{CO,out} + F_{CO_2,out}} \times 100 \quad (2)$$

2.4. Coke analysis

Elemental analysis (EA, CE Instrument) was performed, following the reaction test for 24 h, to measure the amount of coke deposited on the catalyst. Coke was also observed using transmission electron microscopy (TEM, FEI model F20). To obtain the micrographs, 10 mg of the catalysts before and after the reaction test were dispersed in ethanol in an ultrasonic bath for 10 min and subsequently were placed on a copper grid coated with a carbon film.

3. Results and discussion

3.1. Effect of calcination temperature

Fig. 1 shows the methane conversions obtained using the LFN and LCFN, in which the Ce content was 0.3, catalysts at different reaction temperatures. The activity of the LFN catalyst, which was low after calcination at 500 °C (LFN-500), was improved by

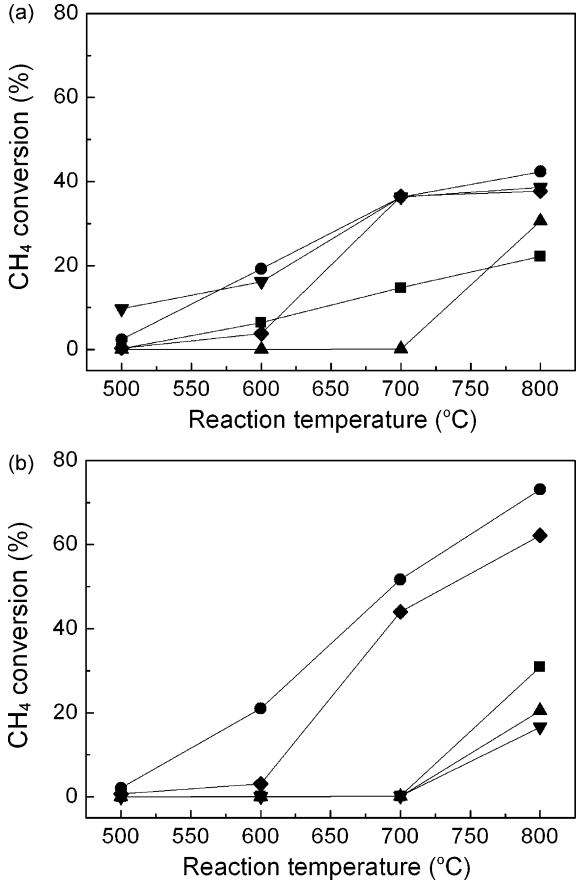

Fig. 1. Effect of calcination temperature on the catalytic activities of LFN (a) and LCFN-0.3 (b) (S/C = 3, GHSV = 86,400 h^{-1}): LFN-500 and LCFN-500 (■); LFN-600 and LCFN-600 (▼); LFN-700 and LCFN-700 (●); LFN-800 and LCFN-800 (◆); LFN-900 and LCFN-900 (▲).

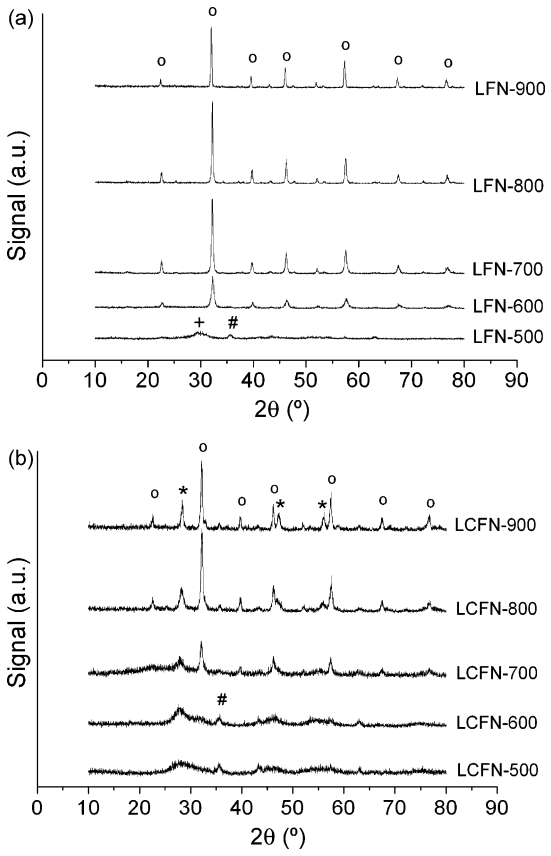

Fig. 2. The XRD patterns of LFN (a) and LCFN-0.3 (b) calcined at temperatures between 500 and 900 °C.

calcination at 600 and 700 °C (LFN-600 and LFN-700), but was lowered by calcination at 800 and 900 °C (LFN-800 and LFN-900). The same trend was observed with the LCFN catalysts, indicating that the activities of LFN and LCFN catalysts were maximized after calcination at 700 °C. Ce-substitution was beneficial to the catalyst performance, as demonstrated by a higher methane conversion for LCFN-700 (73.0% at 800 °C) than for LFN-700 (42.3%). Consequently, 700 °C was selected as the optimal calcination temperature in the subsequent preparation of catalysts.

The X-ray diffraction patterns of LFN (a) and LCFN (b) are displayed in Fig. 2. For the LFN catalysts that were calcined at temperatures above 600 °C, relatively sharp peaks were observed at 32.3°, 46.2° and 57.5° (2θ), which originated from $LaFeO_3$ (JCPDS, 371493) and $LaNiO_3$ (JCPDS, 330711) that underwent lattice contraction by Ni-substitution. These results are consistent with a previous study [26]. LCFN catalysts also showed similar peaks at the same positions when calcined at temperatures higher than 700 °C. Therefore, it was concluded that a well-crystallized perovskite structure formed in the LFN and LCFN catalysts after calcination at temperatures above 600 and 700 °C, respectively. In the cases of LFN-500, LCFN-500 and LCFN-600, which had insignificant activities for the SRM, the perovskite structure was not observed, but phases of LaO (30.1°, JCPDS, 330716) and Fe_2O_3 (35.6°, JCPDS, 391346) were observed for LFN-500 and additionally CeO_2 phase (28.5°, JCPDS, 431002) for LCFN-500 and LCFN-600. The above results suggest that the activity for the SRM was closely related to the formation of perovskite structures in the catalysts. Full-width-at-half-maximum (FWHM) values of the main peak, which was observed at 32.3°, decreased with an increase in the calcination temperature, indicating that the crystallite sizes of LFN and LCFN increased with the calcination temperature.

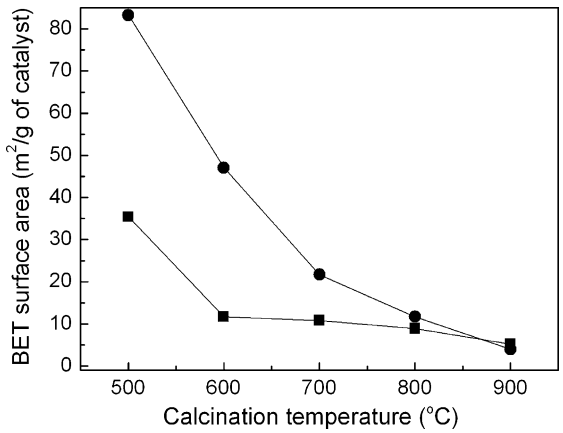

Fig. 3. BET surface areas of LFN (■) and LCFN-0.3 (●).

BET surface areas of LFN and LCFN (Fig. 3), which were respectively 35 and 83 m^2/g after calcination at 500 °C, decreased with calcination temperature to approximately 4 m^2/g for LFN-900 and LCFN-900. This significant decrease in the surface area may explain the inactivity of the latter catalysts.

3.2. Effect of Ce-substitution

Figs. 4 and 5 show the reaction results obtained using LCFN-x under mild (S/C = 3) and severe (S/C = 1) reaction conditions, respectively. In both cases, methane conversion increased with an increase in the amounts of added Ce up to x = 0.2–0.3, but decreased significantly at larger amounts, and eventually was reduced to zero for the La-free CFN. A similar trend was observed for H_2 yield, although the data are not shown here. Accordingly, LCFN-0.2 exhibited the best performance under a severe condition (S/C = 1), while LCFN-0.3 exhibited the best performance under a mild condition (S/C = 3) among the prepared catalysts.

In Table 1, the surface area of LCFN-x increased from 10.8 to 26.2 m^2/g with increasing values of x up to 0.5, but slightly decreased when x was equal to 1.0, i.e., CFN. On the other hand, CO uptake, which was measured for catalysts reduced in H_2/N_2 at 700 °C and therefore represented the amounts of reduced surface-metal components such as Ni and Fe, increased from 0.013 to 0.083 cm^3/g with an increase in x up to 0.2, but decreased to 0.033 cm^3/g when x was equal to 0.5. Previous studies reported that $La_{0.6}Ce_{0.4}Fe_{0.8}Ni_{0.2}O_3$ had a surface area larger than that of $LaFe_{0.8}Ni_{0.2}O_3$ [18] and metal dispersion was enhanced by Ce

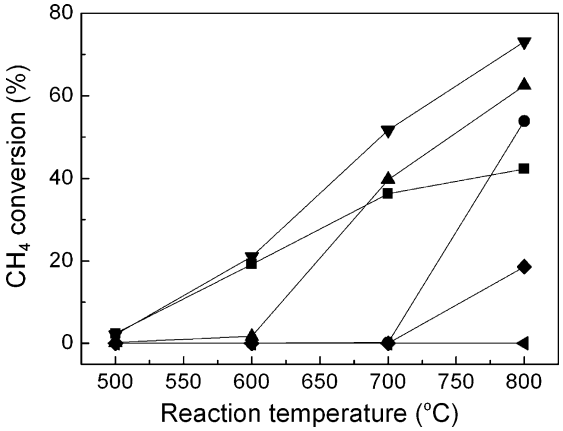

Fig. 4. Effect of Ce-substitution on the catalytic activities of LCFN-x under mild reaction conditions (S/C = 3, GHSV = 86,400 h^{-1}): LFN (■); LCFN-0.1 (●); LCFN-0.2 (▲); LCFN-0.3 (▼); LCFN-0.5 (◆); CFN (◀).

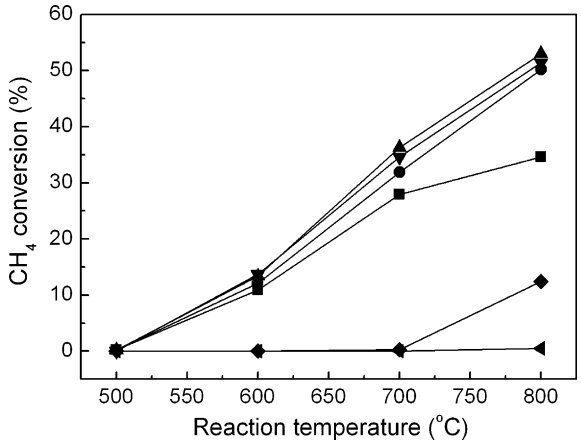

Fig. 5. Effect of Ce-substitution on the catalytic activities of LCFN-*x* under severe reaction conditions (S/C = 1, GHSV = 86,400 h^{-1}): LFN (■); LCFN-0.1 (●); LCFN-0.2 (▲); LCFN-0.3 (▼); LCFN-0.5 (◆); CFN (◀).

Table 1
The textual properties of LCFN-*x*.

Catalyst	S_{BET}	CO uptake[a] (cm^3/g of sample)
LFN	10.8	0.013
LCFN-0.1	8.7	0.024
LCFN-0.2	13.4	0.083
LCFN-0.3	21.7	0.065
LCFN-0.5	26.2	0.033
CFN	21.9	–

[a] Measured by CO chemisorption.

addition [27–30]. Catalytic activity should be affected by changes in surface area and metal dispersion.

The XRD patterns of LCFN-*x*, shown in Fig. 6, indicate that the perovskite structure of the catalysts, represented by diffraction lines at 32.3°, 46.2° and 57.5°, was preserved up to $x = 0.3$. The results also showed the diffraction lines characteristic of a CeO_2 phase, observed at 28.5°, 47.5° and 56.3°, when $x > 0.1$. The above results suggest that the majority of the added Ce substituted for La when $x \leq 0.1$. However, when *x* was larger than 0.1, some of Ce was present as CeO_2. In fact, Lima et al. [14] reported that the perovskite and CeO_2 phases co-existed in $La_{0.95}Ce_{0.05}NiO_3$ due to the limited solubility of Ce in $La_{1-y}Ce_yNiO_3$. In the case of CFN, diffraction lines characteristic of perovskite were not observed, indicating that Ce and Fe existed separately in the forms of CeO_2 and Fe_2O_3. Lines representing NiO were not observed in this study, probably because NiO was present in amounts below the detection limit or in the form of an amorphous phase.

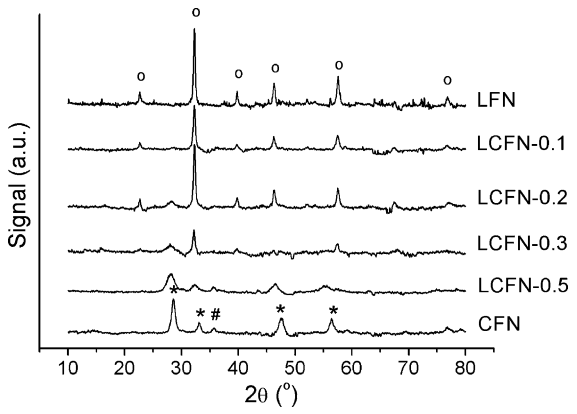

Fig. 6. The XRD patterns of LCFN-*x*: Perovskite (o), CeO_2 (*) and Fe_2O_3 (#).

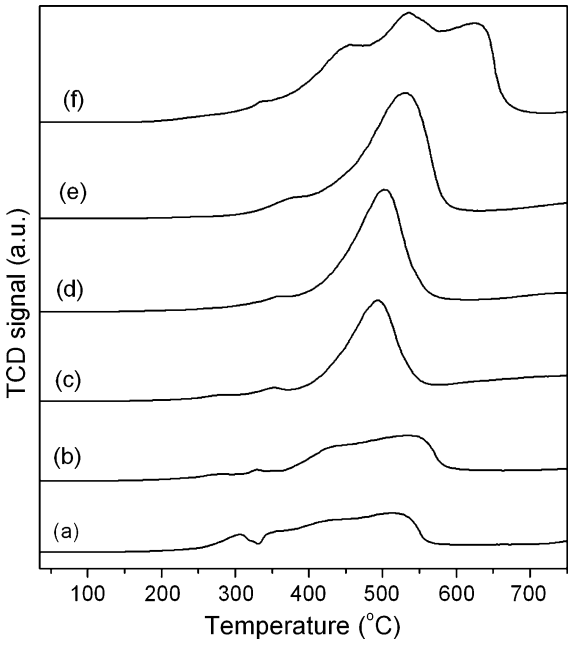

Fig. 7. TPR profiles of LCFN-*x*: (a) LFN; (b) LCFN-0.1; (c) LCFN-0.2; (d) LCFN-0.3; (e) LCFN-0.5; (f) CFN.

Because the active sites of LFN catalysts for the SRM are metallic Ni species, the catalysts must be reduced prior to use in the reaction tests. Fig. 7 shows the results of TPR experiments conducted to examine the reducibility of LCFN-*x* catalysts. In the case of LFN, weak and broad peaks, representing the reduction of Ni^{3+} and Ni^{2+} ions [14,26], were observed in the range of 300 and 550 °C, indicating that the Ni ions incorporated into the perovskite structure were not easily reduced. A similar result was observed when Ce was added in small amounts, as in the case of LCFN-0.1. However, the broad peaks were replaced by an intense peak, centered at 500 °C, when the amount of added Ce increased to $x = 0.2–0.3$, as for LCFN-0.2 and LCFN-0.3. This result indicates that Ni ions were more easily reduced in LCFN-0.2 and LCFN-0.3 than in LFN and LCFN-0.1. A similar trend was reported by Pecchi et al. [26], who observed two hydrogen consumption peaks at 337 and 496 °C in the $LaNiO_3$ perovskite sample, but a single peak in the Fe-substituted $LaFe_{1-y}Ni_yO_3$ ($y = 0.1–0.3$) perovskite.

In the case of LCFN-0.5, the main peak was shifted to temperatures higher than those observed for the LCFN-0.2 and LCFN-0.3 peaks, indicating reduction of the surface CeO_2 species, which were present in excess amounts. It was reported that the surface Ce^{4+} was reduced to Ce^{3+} at 527 °C in $La_{1-y}Ce_yNiO_3$ containing large amounts of added Ce [14]. Finally, in the case of CFN, peaks with significantly different shapes were observed. New peaks observed at approximately 450 and 630 °C probably originated from the reduction of NiO [31] and Fe_2O_3 [32], respectively, which were identified in the XRD pattern of the CFN catalyst.

3.3. LCFN-0.2 versus the COM

Fig. 8 shows the fractional amounts of H_2 produced using LCFN-0.2 and a COM at 700 °C and different S/C ratios. The H_2 fraction obtained using COM decreased significantly from 79 to 51.9% when the S/C ratio was reduced from 3 to 1, while that obtained using LCFN-0.2 remained relatively insensitive to the S/C ratio. Consequently, the H_2 fractions were greater for the latter catalyst than for the former at S/C ratios less than 1.5.

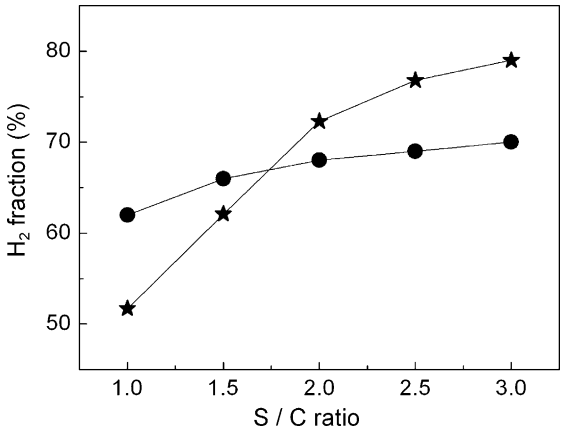

Fig. 8. H_2 fraction obtained using LCFN-0.2 (●) and COM (★) for various S/C ratios at 700 °C.

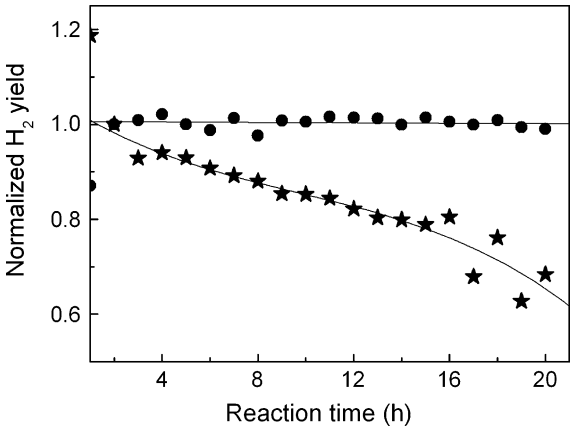

Fig. 9. Changes in the catalyst activity as a function of the reaction time (S/C = 1, temperature = 700 °C): LCFN-0.2 (●); COM (★).

The deactivation behaviors of LCFN-0.2 and COM were compared based on the results of long-term tests conducted at 700 °C and a S/C ratio of 1 for 20 h. Fig. 9 shows that the H_2 yield, which was normalized to the initial one, decreased rapidly for COM, but remained unchanged for LCFN-0.2 over a reaction period of 20 h, indicating that the latter catalyst was more tolerant to deactivation than the former.

The amount of coke deposited on the catalysts after 20 h of use, estimated by EA, was 48.7 wt.% for COM and 0.2 wt.% for LCFN-0.2. This result was also supported by the TEM results, Fig. 10, that showed an abundance of carbon whiskers and filaments on the surface of the used COM. Accordingly, the carbon species that formed on LCFN-0.2 during the SRM were readily gasified, while those on COM accumulated on the surface to eventually form filamentous materials. In the case of LCFN-*x*, lattice oxygen vacancies that were generated by Ce-substitution in the perovskite structure might be responsible for gasification of the carbon species because the vacancies acted as active sites for the

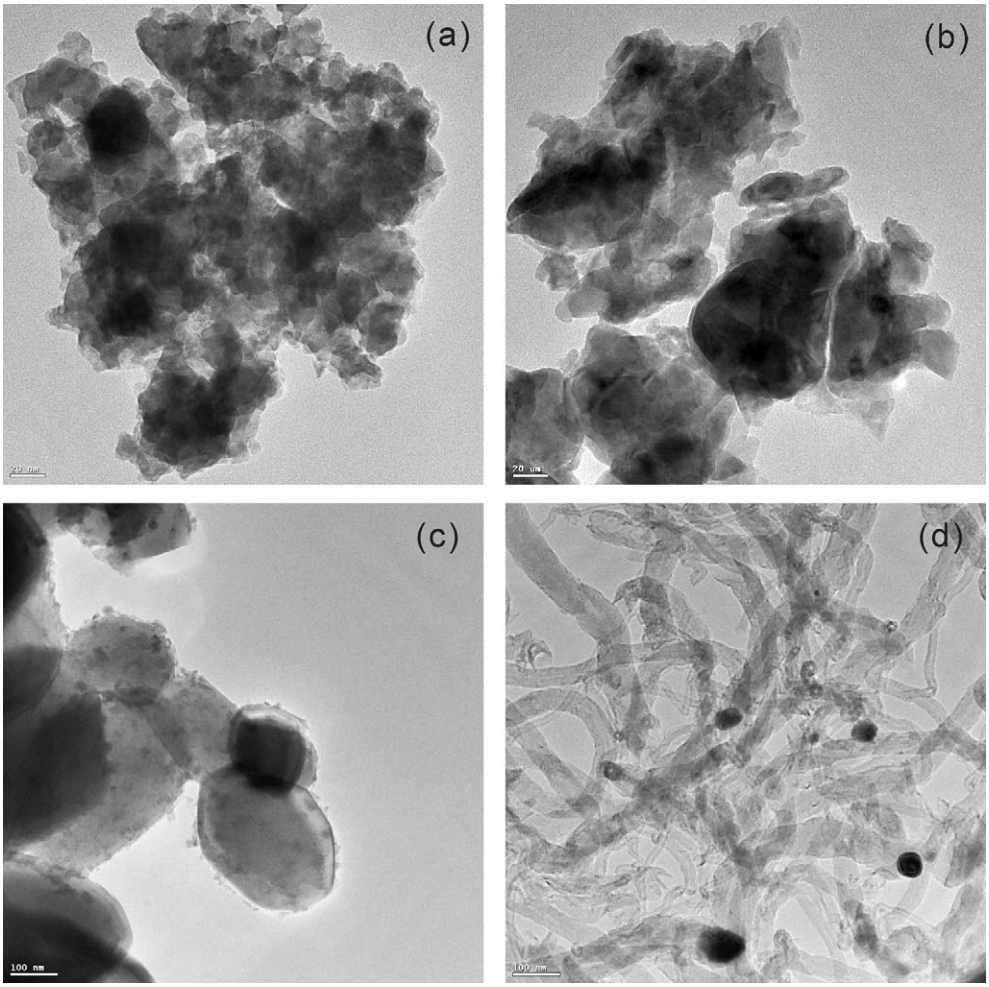

Fig. 10. TEM images of LCFN-0.2 (a and b) and COM (c and d) obtained before and after the reaction test.

dissociation of steam under the reaction condition used in the present study. CeO_2 that was present in the LCFN-x catalysts, particularly as small particles when $x < 0.3$, might also contribute to the improved tolerance of the catalyst to coking by storage and provision of the oxygen that was necessary for gasification of the carbon species.

4. Conclusions

In this study, Ce-substituted $LaFe_{0.7}Ni_{0.3}O_3$ perovskite catalysts were prepared using a Pechini method and the effects of both the calcination temperature and Ce-substitution on the structure and performance of the catalysts in SRM were investigated. The following conclusions can be drawn based on the results of both the reaction test and catalyst characterization:

1. Perovskite structures of LFN and LCFN formed after calcination at temperatures higher than 600 and 700 °C, respectively. Under the reaction conditions examined in this study, 700 °C was determined to be the optimal calcination temperature to obtain the best catalytic performance.

2. Ce-substitution enhances the methane conversion and H_2 fraction by increasing both the BET surface area and the metal dispersion. Ce-substitution also retards coke deposition due to the enhanced coke gasification by lattice oxygen. In particular, $La_{0.8}Ce_{0.2}Fe_{0.7}Ni_{0.3}O_3$ (LCFN-0.2) exhibited a higher hydrogen fraction and slower deactivation rates than those exhibited by a COM, when the S/C ratio of the reactant stream was less than 1.5.

Acknowledgements

This study was supported by GS Caltex Corp., Brain Korea 21 (BK21) project, National Research Laboratory (NRL) program and the Center for Ultramicrochemical Process systems (CUPS).

References

[1] P. Ferreira-Aparicio, M.J. Benito, Catal. Rev. 47 (2005) 491.
[2] J.R. Rostup-Nielsen, J. Sehested, J.K. Norskov, Adv. Catal. 47 (2002) 65.
[3] A.P. Simpson, A.E. Lutz, Int. J. Hydrogen Energy 32 (2007) 4811.
[4] J.R. Rostup-Nielsen, J. Catal. 33 (1974) 184.
[5] S.D. Jackson, S.J. Thomson, G. Webb, J. Catal. 70 (1981) 249.
[6] D. Duprez, M.C. Demicheli, P. Marecot, J. Barbier, O.A. Ferretti, E.N. Ponzi, J. Catal. 124 (1990) 324.
[7] J. Xu, C.M.Y. Yeung, J. Ni, F. Meunier, N. Acerbi, M. Fowles, S.C. Tsang, Appl. Catal. A 345 (2008) 119.
[8] T. Sperle, D. Chen, R. Lødeng, A. Holmen, Appl. Catal. A 282 (2005) 195.
[9] H.S. Roh, K.W. Jun, W.S. Dong, J.S. Chang, S.E. Park, Y.I. Joe, J. Mol. Catal. A 181 (2002) 137.
[10] K. Urasaki, K. Tokunaga, Y. Sekine, M. Matsukata, E. Kikuchi, Catal. Commun. 9 (2008) 600.
[11] K. Urasaki, Y. Sekine, S. Kawabe, E. Kikuchi, M. Matsukata, Appl. Catal. A 286 (2005) 23.
[12] G.S. Gallego, F. Mondragón, J. Barrault, J.M. Tatibouët, C.B. Dupeyrat, Appl. Catal. A 311 (2006) 164.
[13] J.R. Mawdsley, T.R. Krause, Appl. Catal. A 334 (2008) 311.
[14] S.M. Lima, J.M. Assaf, M.A. Peña, J.L.G. Fierro, Appl. Catal. A 311 (2006) 94.
[15] G. Valderrama, M.R. Goldwasser, C.U. de Navarro, J.M. Tatibouët, J. Barrault, C.B. Dupeyrat, F. Martínez, Catal. Today 107–108 (2005) 785.
[16] A.L. Sauvet, J.T.S. Irvine, Solid State Ionics 167 (2004) 1.
[17] H. Provendier, C. Petit, A. Kiennemann, C.R. Acad. Sci. Paris, Série IIc, Chim./Chem. 4 (2001) 57.
[18] P. Erri, P. Dinka, A. Varma, Chem. Eng. Sci. 61 (2006) 5328.
[19] J. Guo, H. Lou, Y. Zhu, X. Zheng, Mater. Lett. 57 (2003) 4450.
[20] G. Valerrama, A. Kiennemann, M.R. Goldwasser, Catal. Today 133–135 (2008) 142.
[21] N. Yamazoe, Y. Teraoka, Catal. Today 8 (1990) 175.
[22] M.A. Peña, J.L.G. Fierro, Chem. Rev. 101 (2001) 1981.
[23] D.D. Sarma, A. Chainani, J. Solid State Chem. 111 (1994) 208.
[24] M.P. Pechini, US Patent No. 3,330,697.
[25] A. Worayingyong, P. Kangvansura, S. Ausadasuk, P. Praserthdam, Colloid Surf. A: Physicochem. Eng. Aspects 315 (2008) 217.
[26] G. Pecchi, P. Reyes, R. Zamora, L.E. Cadús, J.L.G. Fierro, J. Solid State Chem. 181 (2008) 905.
[27] S. Eriksson, S. Rojas, M. Boutonnet, J.L.G. Fierro, Appl. Catal. A 326 (2007) 8.
[28] K.-W. Jun, H.-S. Roh, K.V.R. Chary, Catal. Surv. Asia 11 (2007) 97.
[29] H.-S. Roh, K.Y. Koo, U.D. Joshi, W.L. Yoon, Catal. Lett. 125 (2008) 283.
[30] H.-S. Roh, H.S. Potdar, K.-W. Jun, J.-W. Kim, Y.-S. Oh, Appl. Catal. A 276 (2004) 231.
[31] X. Cai, X. Dong, W. Lin, J. Nat. Gas Chem. 17 (2008) 98.
[32] L. Kongzhai, W. Hua, W. Yonggang, L. Mingchun, J. Rare Earths 26 (2008) 245.